ELSEVIER

Polymer 40 (1999) 2687–2698

polymer

Interaction energies for blends of SAN with methyl methacrylate copolymers with ethyl acrylate and *n*-butyl acrylate

J.H. Chu, D.R. Paul*

Department of Chemical Engineering and Center for Polymer Research, The University of Texas at Austin, Austin, TX 78712, USA

Received 6 May 1998; revised 16 June 1998; accepted 23 June 1998

Abstract

Isothermal miscibility maps for blends of styrene–acrylonitrile (SAN) copolymers with methyl methacrylate (MMA) copolymers containing ethyl acrylate (EA) and *n*-butyl acrylate (nBA) have been determined. The miscibility region for MMA-nBA copolymers is larger than that for MMA-EA copolymers. Binary interaction energies for monomer unit pairs were calculated from critical molecular weight experiments and data from the miscibility maps using with the Flory–Huggins theory combined with the binary interaction model. Spinodal temperatures predicted from the lattice-fluid theory of Sanchez and Lacombe, using these experimental interaction energies, are similar to the experimental phase separation temperatures.

Keywords: Blends; Methyl methacrylate copolymers; Styrene–acrylonitrile copolymers

1. Introduction

The energetic interaction between unlike polymer pairs is a fundamental thermodynamic issue that governs the state of miscibility of their blends or the nature of the interface between domains when the blend is phase separated. It is, therefore, crucial to quantify these interactions, and this work contributes to a growing base of polymer–polymer interaction energies for use in the rational design of multicomponent polymer systems. One approach to obtaining this information is to observe the boundaries (molecular weight, copolymer composition, temperature) that divide miscible from immiscible blends and interpret these results within the framework of an appropriate thermodynamic theory.

Blends of poly(methyl methacrylate) (PMMA) with styrene–acrylonitrile copolymers (SAN) form miscible blends within a well-defined range of AN content and temperature [1–7]. Thus, copolymers of methyl methacrylate with another monomer X must have some region of miscibility with SAN copolymers and several such systems have been studied previously in this laboratory. For example, Nishimoto et al. [7] investigated blends of SAN copolymers with methyl methacrylate copolymerized with cyclohexyl methacrylate, CHMA, phenyl methacrylate, PhMA, and tert-butyl methacrylate, tBMA. Gan and Paul [8–10] also examined blends of SAN copolymers with MMA-tBMA and methyl methacrylate-glycidyl methacrylate copolymers, MMA-GMA. By mapping the regions of AN and X comonomer compositions that divide miscible from immiscible blends at a fixed temperature and molecular weight of the components, it is possible to obtain some information about the binary interaction energies between the various repeat unit pairs. This paper continues the use of this strategy to gain further knowledge about polymer–polymer interactions for systems of some technological significance.

Methacrylate polymers are notorious for their tendency to depolymerize by an unzipping mechanism at temperatures near those used in processing. However, acrylate polymers have much higher ceiling temperatures and do not unzip at normal processing temperatures. Thus, small amounts of an acrylate comonomer are incorporated in commercial MMA-based polymers to increase their stability against depolymerization. Therefore, it is important to understand the effect of the acrylate content of MMA-based polymers on their miscibility with other polymers. Ethyl acrylate (EA) and *n*-butyl acrylate (nBA) are typical acrylates used for this purpose and were chosen for this study of blends of MMA-X copolymers with SAN copolymers.

2. Theory

Three approaches to obtaining interaction energy information will be used in this study, and all require the use of

* Corresponding author. Tel.: +1-512-471-5392; Fax: +1-512-471-0542; E-mail: drp@che.utexas.edu

0032-3861/99/$ - see front matter
PII: S0032-3861(98)00499-6

an appropriate thermodynamic theory of mixing. The simplest theory for polymer mixtures is that of Flory and Huggins [11,12] which gives the free energy of mixing for a blend of polymers A and B as

$$\Delta g_{\text{mix}} = B\phi_A\phi_B + \text{RT}\left[\frac{\rho_A \ln \phi_A}{M_A} + \frac{\rho_B \ln \phi_B}{M_B}\right], \quad (1)$$

where R is the universal gas constant, T is the absolute temperature, and ϕ_i, ρ_i, and M_i are the volume fraction, density, and molecular weight of component i, respectively. According to the binary interaction model [13–15], the interaction energy density B of a polymer blend involving copolymers can be expressed in terms of interactions between the various pairs of monomer units present and their volume fraction in the copolymer. For a blend of copolymer A, consisting of monomers 1 and 2, and copolymer B, consisting of monomers 3 and 4, this expression is

$$B = B_{13}\phi_1'\phi_3'' + B_{14}\phi_1'\phi_4'' + B_{23}\phi_2'\phi_3'' + B_{24}\phi_2'\phi_4'' - B_{12}\phi_1'\phi_2' - B_{34}\phi_3''\phi_4'', \quad (2)$$

where ϕ_i' is the volume fraction of monomer i in the copolymer A, ϕ_j'' is the volume fraction of monomer j in copolymer B, and B_{ij} is the interaction between monomer units i and j. Isothermal miscibility mapping in conjunction with Eq. (2) is one method of obtaining information about the various B_{ij} values.

Kambour et al. [14], and Callaghan and Paul [16,17], have used a critical molecular weight method for determining positive interaction energies. The molecular weights of the immiscible component polymers are reduced until the blend becomes miscible due to the dominance of the favorable contribution of the entropy of mixing over the unfavorable enthalpy of mixing. The critical interaction energy at this boundary between miscibility and immiscibility is given by the following equation

$$B_{\text{crit}} = \frac{\text{RT}_c}{2}\left[\sqrt{\frac{\rho_A}{(\bar{M}_w)_A}} + \sqrt{\frac{\rho_B}{(\bar{M}_w)_B}}\right]^2. \quad (3)$$

A third approach to evaluating interaction energies is a quantitative analysis of the phase diagram; polymer blends often exhibit phase separation on heating or a lower critical solution temperature (LCST). The Flory–Huggins theory assumes incompressibility of the polymer mixture; therefore, it is unable to predict LCST behavior in a simple way. Equation-of-state (EOS) theories, such as the lattice-fluid theory proposed by Sanchez and Lacombe [18–22], include compressibility and naturally predict LCST behavior. The lattice-fluid equations are expressed in terms of reduced pressure, temperature, and density (or volume), i.e. $\tilde{P} = P/P*$, $\tilde{T} = T/T*$, $\tilde{\rho} = 1/\tilde{v} = \rho/\rho*$, where the variables with asterisks are characteristic parameters. The characteristic parameters are calculated by fitting experimental PVT data of the homopolymers to the lattice-fluid equation-of-state and using mixing rules for copolymers. Because the mathematical form of the equation-of-state does not perfectly fit the experimental PVT data for polymers, the parameters obtained depend to some degree on the details of the curve fitting process and especially the temperature range of the PVT data used. The significance of this fact becomes evident in later discussions.

The characteristic pressure of the mixture $P*$ is related to the bare interaction energy $\Delta P*$:

$$P* = \phi_1 P_1^* + \phi_2 P_2^* - \phi_1\phi_2\Delta P^*, \quad (4)$$

where P_i* is the characteristic pressure of the component i. The bare interaction energy can be related to the Flory–Huggins interaction energy density at the spinodal condition as follows [23,24]:

$$B_{sc} = \tilde{\rho}\Delta P^* + \left\{[P_2^* - P_1^* + (\phi_2 - \phi_1)\Delta P^*] + \frac{\text{RT}}{\tilde{\rho}}\left(\frac{1}{r_1^o v_1*} - \frac{1}{r_2^o v_2*}\right) - \text{RT}\left(\frac{\ln(1-\tilde{\rho})}{\tilde{\rho}^2} + \frac{1}{\tilde{\rho}}\right)\left(\frac{1}{V_1^*} - \frac{1}{V_2^*}\right)\right\}^2 / \times\left\{\frac{2RT}{v*}\left[\frac{2\ln(1-\tilde{\rho})}{\tilde{\rho}^3} + \frac{1}{\tilde{\rho}^2(1-\tilde{\rho})} + \frac{(1-1/r)}{\tilde{\rho}^2}\right]\right\} \quad (5)$$

where r is the chain length and $v*$ is the characteristic hard core volume per mer. Thus, by comparing experimental phase separation temperatures of the LCST type to the lattice-fluid theory, information about the interaction energy density of a blend can be obtained.

3. Materials and procedures

Methyl methacrylate and *n*-butyl acrylate monomers were washed with an aqueous sodium hydroxide solution, rinsed with distilled water, and dried over calcium chloride. Ethyl acrylate was used as received. Polymerization was performed in bulk at 60°C with AIBN as the initiator. Polymer was recovered using an excess of methanol and was purified using chloroform/methanol reprecipitation. Conversion was kept less than 10% to avoid composition drift in the copolymer.

Table 1
Acrylic polymers synthesized for this study

Abbreviation	Wt% Acrylate	$\bar{M}_n$	$\bar{M}_w$	T_g (°C)
PMMA	0	116 000	217 500	117
MMA-EA3	3	143 000	283 700	110
MMA-EA8	8	142 100	279 500	108
MMA-EA10	10	162 000	309 000	101
MMA-EA12	12	146 300	291 800	91
MMA-EA13	13	152 800	304 400	87
MMA-EA15	15	159 700	308 300	84
MMA-EA22	22	166 000	326 000	74
MMA-nBA7	6.9	172 700	374 400	106
MMA-nBA13	13	187 600	404 400	83
MMA-nBA18	18	205 500	413 500	65
MMA-nBA27	27	187 700	336 700	59
MMA-nBA32	32	167 600	314 000	48
MMA-nBA35	35	154 900	300 900	43
MMA-nBA40	40	205 500	413 500	35
PEA	100	34 500	395 000	− 17

Table 2
SAN copolymers used in this study

Polymer	wt% AN	$\bar{M}_n$	$\bar{M}_w$	Source
SAN3.5	3.8	93 000	204 000	Asahi Chemical
SAN6.3	6.3	121 000	343 000	Dow Chemical Co.
SAN9.5	10.0	94 700	195 600	Asahi Chemical
SAN11.5	12.9	68 300	151 400	Asahi Chemical
SAN13.5	15.2	56 300	149 000	Asahi Chemical
SAN15.5	17.7	65 300	144 300	Asahi Chemical
SAN16	15.9	–	173 900	Dow Chemical Co.
SAN19.5	20.8	84 300	178 700	Asahi Chemical
SAN23	23	43 300	117 500	Daicel Chemical Ind. Ltd.
SAN25	25	77 000	152 000	Dow Chemical Co.
SAN28	28.4	52 900	143 800	Asahi Chemical
SAN30	30	81 000	168 000	Dow Chemical Co.
SAN33	33	68 000	146 000	Monsanto Co.

The polymers synthesized in this study are described in Table 1. The comonomer content of synthesized polymers was determined by ^{1}H NMR. Molecular weight information was obtained using gel permeation chromatography calibrated with polystyrene standards. These copolymers were blended with the various SAN copolymers, listed in Table 2. Table 3 contains information about the polymer standards used in critical molecular weight experiments. All blends were solution cast from dichloromethane at room temperature, then dried under vacuum while increasing the temperature 30°C every day until 120°C. Glass transition temperatures were determined using a Perkin-Elmer DSC-7 at a scanning rate of 20°C/min. A first scan was run to 120°C to erase thermal history and a second scan was run for analysis. Fig. 1 shows the onset glass transition temperatures for the synthesized copolymers. As the glass transition temperatures of the copolymers were too close to observe blend miscibility using DSC, phase behavior was determined visually. Phase separation temperatures were determined using a Mettler FP82HT Hot Stage equipped with a Mettler FP80HT Central Processor. A Gnomix PVT apparatus was used to obtain PVT data for PnBA from which the characteristic Sanchez–Lacombe equation-of-state parameters were calculated.

Table 3
Polymer standards used in this study

Polymer	$\bar{M}_n$	$\bar{M}_w/\bar{M}_n$	Source
PS 580	580	1.18	Polymer Laboratories
PS 800	800	1.30	Pressure Chemical
PS 2000	2000	1.06	Pressure Chemical
PS 4000	4000	< 1.06	Pressure Chemical
PS 9000	9000	< 1.06	Pressure Chemical
PS 17 500	17 500	1.04	Pressure Chemical
PS 30 300	30 300	1.03	Polymer Laboratories
PS 400 000	400 000	≤ 1.06	Pressure Chemical
PMMA 1210	1210	1.16	Polymer Laboratories
PMMA 4250	4250	1.07	Polymer Laboratories
PMMA 10 550	10 550	1.11	Polymer Laboratories
PMMA 20 300	20 300	1.11	Polymer Laboratories
PMMA 265 600	265 600	≤ 1.14	Pressure Chemical
PnBA	$\overline{M}_w = 101\,000$	2.66	Aldrich Chemical

4. Discussion of previously determined interaction energies

A complete description of the phase behavior for the blends of styrene–acrylonitrile (SAN) copolymers with methyl methacrylate copolymers requires knowledge about six different binary interaction energies for each set of blends, as seen in Eq. (3). There are three common interaction energies for all blends of this type, viz., $B_{S/AN}$, $B_{MMA/AN}$, and $B_{S/MMA}$, which have been evaluated previously in other studies [8,16,25–32]; those results will be discussed here.

In Figs 2 and 3, experimental values of B_{ij} from the literature are plotted as a function of the temperature at which they were determined. These data were obtained using various methods, such as concentrated ternary solution measurements [25–27], small angle neutron scattering [28], critical molecular weight technique [16], and copolymer

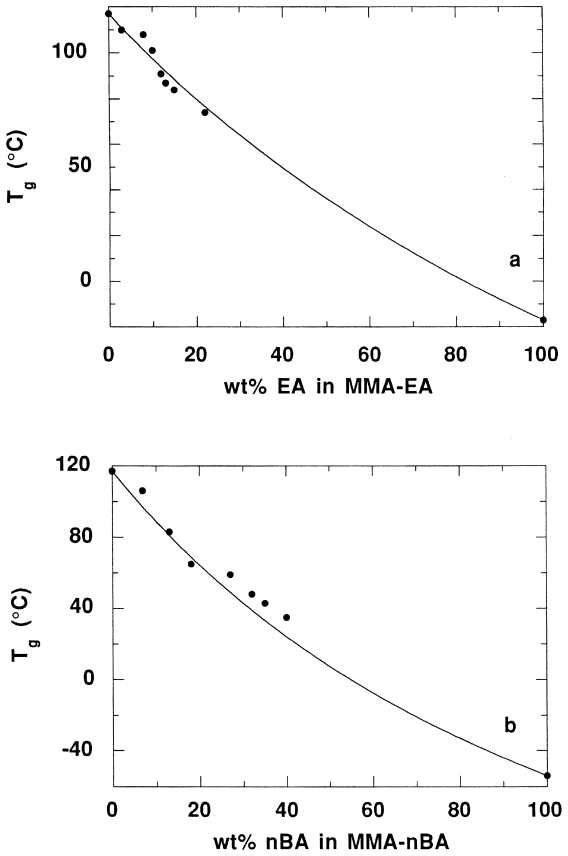

Fig. 1. Glass transition temperatures for synthesized copolymers determined by DSC (onset method) at 20°C/min: (a) MMA-EA copolymers; (b) MMA-nBA copolymers.

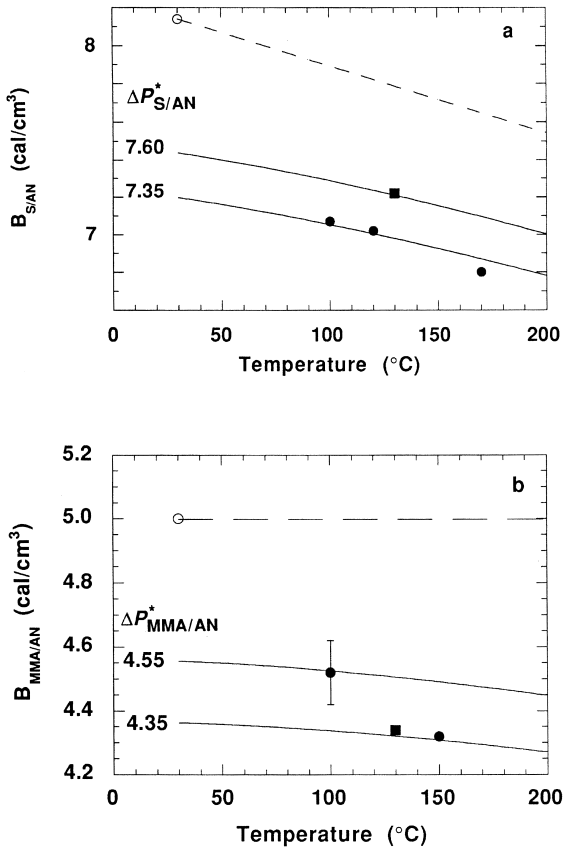

Fig. 2. B_{ij} values as a function of temperature using characteristic parameters calculated directly from experimental data for the temperature range 150°C–200°C: (a) $B_{S/AN}$; (b) $B_{MMA/AN}$. The solid curves were calculated for the value of ΔP^* shown. The dashed curves are those proposed by Brannock [29]. The data are from (○) Brannock [29]; (•) Gan [8,30,31]; and (■) Nishimoto [32].

miscibility boundaries [8,29–32]. The solid curves were calculated from Eq. (5) using the characteristic parameters found in Table 4 and the values of ΔP^* shown. The ΔP^* values were selected so that the curves would roughly bracket the data. The dotted curves show the values proposed by Brannock et al. [29]. In the plots for $B_{S/AN}$ [Fig. 2(a)] and $B_{MMA/AN}$ [Fig. 2(b)] the temperature range of the characteristic parameters used to calculate the curves was 150°C–200°C, which corresponds well to the experimental temperatures used in this study. In Fig. 2, these curves and the ones suggested by Brannock have similar shapes and follow the trends shown by the data. The fact that the temperature dependence of these Flory–Huggins based interaction energies is well-described by the Sanchez–Lacombe theory with constant ΔP^*_{ij} suggests that the origin of the temperature dependence lies in equation-of-state effects.

Table 4
Sanchez–Lacombe characteristic parameters used in this study

Polymer	T^*(K)	P^*(MPa)	ρ^*(g cm^{-3})	Temperature range (°C)	Reference
PS	751	397.0	1.109	150–200	[31]
PS	810	373.0	1.092	220–270	[31]
PMMA	728	503.0	1.2601	150–200	[33]
PMMA	742	509.0	1.2564	220–270	[33]
PAN	853	535.7	1.2299	150–200	[33]
PEA	640	401.4	1.1857	37–217	[34]
PnBA	646	378.8	1.1459	150–210	this study

The corresponding plot for $B_{S/MMA}$ is shown in Fig. 3(a). The curves calculated using equation-of-state parameters evaluated over the temperature range of 150°C–200°C do not agree well with the temperature dependence of the experimental $B_{S/MMA}$ values from the literature, i.e. the data seems to have a positive temperature slope while the calculated curves have a slight negative slope. However, when using characteristic parameters evaluated over the temperature range of 220°C–270°C, which differ slightly from the characteristic parameters corresponding to the previous temperature range as seen in Table 4, the calculated curves have a slope similar to that of the experimental data, as shown in Fig. 3(b). Thus, the temperature range over which the EOS parameters are evaluated can have an important effect on the predicted temperature dependence of the Flory–Huggins interaction energy, B_{ij}, in some cases.

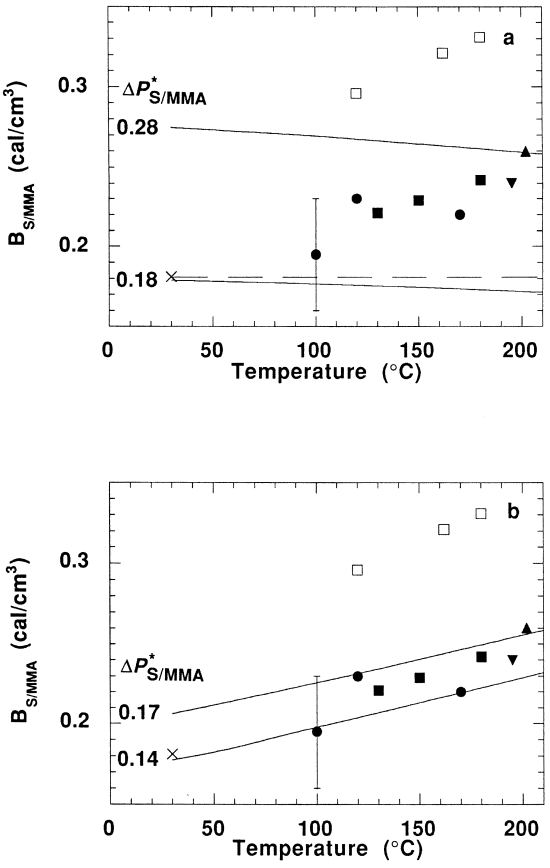

Fig. 3. $B_{S/MMA}$ as a function of temperature using characteristic parameters calculated for the temperature ranges: (a) 150°C–200°C; and (b) 220°C–270°C. The solid curves were calculated for the value of ΔP^* shown. The dashed curves are those proposed by Brannock [29]. The data are from (▲) Callaghan [16]; (×) Fukuda [25–27]; (•) Gan [8,30,31]; (▼) Massa [16]; (■) Nishimoto [32]; and (□) Russell [16,28].

Table 5
Results from critical molecular weight experiments using PEA

PS molecular weight	Film appearance	$B_{S/EA}$ (cal/cm^3)	PMMA molecular weight	Film appearance	$B_{MMA/EA}$ (cal/cm^3)
400 000	cloudy	> 0.0042	265 600	cloudy	> 0.0055
30 300	cloudy	> 0.022	20 300	cloudy	> 0.033
17 500	cloudy	> 0.034	10 550	cloudy	> 0.058
9 000	cloudy	> 0.060	4 250	clear	< 0.13
4 000	cloudy	> 0.12	1 210	clear	< 0.41
2 000	cloudy	> 0.23			
800	cloudy	> 0.56			
580	cloudy	> 0.76			

To better understand the predicted temperature dependence of B, the components of Eq. (5) used to develop the curves shown in Figs 2 and 3 must be examined more closely. This equation consists of two basic parts: the first term containing the bare interaction energy, and the remaining terms in the brackets which account for the equation-of-state effects. Values for these two parts of the equation were calculated for the various interaction pairs using characteristic parameters evaluated over different temperature ranges in the PVT data. It was found for a given ΔP^* that the first term, $\tilde{\rho}\Delta P^*$, decreases with temperature; whereas, the group of remaining terms generally increases with temperature. For large values of ΔP^*, the second term is not significant; however, for small values of ΔP^* the second term can be significant enough to change the slope. Thus, for most B_{ij}, the first term dominates and there is an overall increase with temperature. However, with $B_{S/MMA}$ the magnitudes are small enough that the second term of Eq. (5) can become dominant and slight differences in the characteristic parameters can cause significant changes in the predicted temperature dependence of $B_{S/MMA}$. The values used in this study were chosen using the characteristic parameters from the logical temperature range of 150°C–200°C.

5. Critical molecular weight experiments

There are three remaining binary interaction energies for each of the current blend systems: $B_{S/EA}$, $B_{MMA/EA}$, and $B_{EA/AN}$ for the MMA-EA/SAN blends, and $B_{S/nBA}$, $B_{MMA/nBA}$, and $B_{nBA/AN}$ for the MMA-nBA/SAN blends. In principle, information about the interaction of styrene, S, and methyl methacrylate, MMA, units with each of these acrylate monomer units, EA or nBA, can be obtained by the so-called critical molecular weight technique [14,16,17]. For some immiscible polymer pairs, decreasing the molecular weight of one or both components can lead to miscibility; thus, Eq. (3) can be used to calculate the interaction energy from these observed critical molecular weights that define the boundary between miscibility and immiscibility. Blends of high molecular weight homopolymers of PEA and PnBA with homopolymers of PS and PMMA of various molecular weights were used in such experiments; the results are shown in Tables 5 and 6. Since the necessary polyacrylonitrile polymers are not available, this approach could not be used to obtain information about $B_{EA/AN}$ or $B_{nBA/AN}$.

Blends of PEA with monodisperse polystyrenes with molecular weights ranging from 580 to 400 000 were all found to be immiscible. This indicates that $B_{S/EA}$ is greater than 0.76 cal/cm^3. Blends of PEA with PMMA polymers having $\overline{M}_n = 10\,500$ and higher were cloudy, but those with molecular weights below 4250 were clear, which suggests $0.058 < B_{MMA/EA} < 0.13$ cal/cm^3. Cowie et al. [35] also obtained miscibility data using blends of PMMA with PEA of various molecular weights. Evaluating these data in the same manner using Eq. (3), gives $B_{MMA/EA} = 0.13$ cal/cm^3, which is similar to the findings in this study.

Blends of PnBA with PS having $\overline{M}_n = 2000$ and higher were all immiscible, but the blend with PS having $\overline{M}_n = 800$ was found to be miscible; thus, $0.27 < B_{S/nBA} < 0.61$. Blends of PnBA with PMMA having molecular weights greater than 4250 were cloudy; however, the PnBA blend with PMMA having $\overline{M}_n = 1,210$ were clear, which leads to $0.15 < B_{MMA/nBA} < 0.46$. This information is useful in conjunction with the isothermal miscibility maps described below for determining values of all relevant binary interaction energies.

Table 6
Results from critical molecular weight experiments using PnBA

PS molecular weight	Film appearance	$B_{S/nBA}$ (cal/cm^3)	PMMA molecular weight	Film appearance	$B_{MMA/nBA}$ (cal/cm^3)
9000	cloudy	> 0.077	10 550	cloudy	> 0.074
4000	cloudy	> 0.15	4 250	cloudy	> 0.15
2000	cloudy	> 0.27	1 210	clear	< 0.46
800	clear	< 0.61			

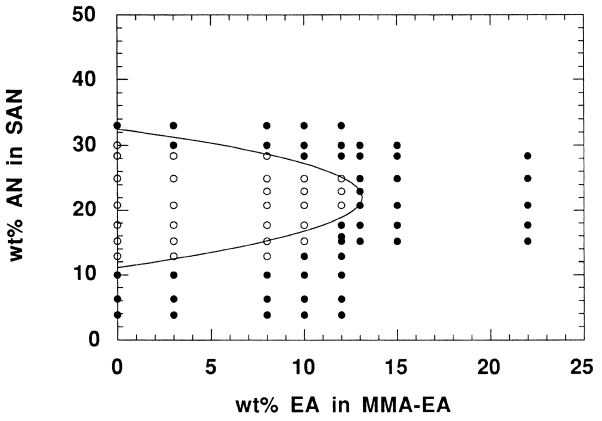

Fig. 4. Copolymer miscibility map at 120°C for 50/50 wt% blends of MMA-EA copolymers with SAN copolymers: (◦) miscible; (•) immiscible. The solid curve was calculated from the B_{ij} set obtained from the best fit of the miscibility map (see Table 7 for values).

6. Isothermal miscibility maps and evaluation of interactions

Copolymer composition miscibility maps for MMA-EA/SAN and MMA-nBA/SAN blends at 120°C are shown in Figs 4 and 5, respectively; both systems show a closed loop region of miscibility. Miscibility of pure PMMA is observed with SAN copolymers containing between 12.9 and 30 wt% AN as reported previously [1–7]. The addition of acrylate comonomer causes the AN limits to narrow and eventually vanish. MMA-EA copolymers containing 13 wt% EA or greater were immiscible with all SAN copolymers. The miscibility region for MMA-nBA/SAN blends is also a closed loop, but it includes a larger acrylate range as shown in Fig. 5. Some region of miscibility was found for all blends with MMA-nBA copolymers containing up to 35 wt% nBA, while the copolymer containing 40% nBA was found to be immiscible with all SAN copolymers. In contrast to EA, addition of nBA tends to skew the miscible region towards lower AN content of the SAN copolymer. These

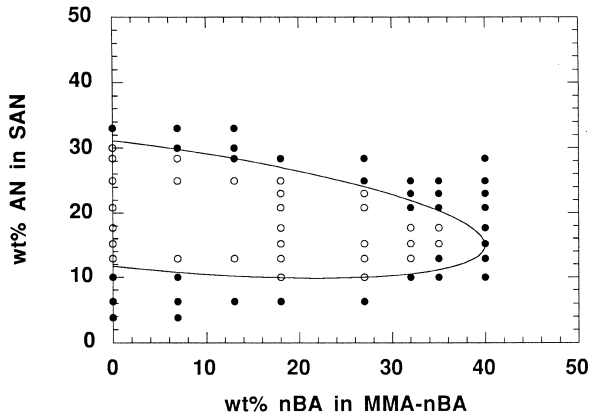

Fig. 5. Copolymer miscibility map at 120°C for 50/50 wt% blends of MMA-nBA copolymers with SAN copolymers: (◦) miscible; (•) immiscible. The solid curve was calculated from the B_{ij} set obtained from the best fit of the miscibility map (see Table 7 for values).

results show that the low levels of acrylate, either EA or nBA, content used in commercial PMMA materials should have minimal effect on the region of miscibility with SAN copolymers.

A set of interaction energies for each blend system can be obtained by fitting Eqs. (2) and (3) to the miscibility maps; however, values for at least one of the six B_{ij} required for each system must be fixed [9]. Since there is extensive data available in the literature for the S/MMA pair and it is one of the three pairs common to both systems, $B_{S/MMA}$ was selected to be the fixed parameter, and the value of 0.22 cal/cm^3 determined at 120°C by Gan and Paul [30] was selected for this purpose.

To fit the theory to the experimental miscibility maps requires a B_{crit} value, defined by Eq. (3), for each blend system. Since the molecular weight varies some among the various copolymers, the actual B_{crit} value is not strictly the same for each blend composition as shown in Fig. 6. The unshaded boxes represent miscible blends, while the shaded boxes indicate immiscible blends. The average B_{crit} value for the MMA-EA/SAN blends along the miscibility border is 0.0085 cal/cm^3 and the average value for the corresponding MMA-nBA/SAN blends is 0.0076 cal/cm^3. Deviations from the average B_{crit} value must be considered in the fitting of interaction parameters determined in this manner.

A computer program was written to determine the set of interaction energies [see Eq. (2)] which best fit the experimental data to the Flory–Huggins based criteria for miscibility. The user specifies an upper and lower limit for each interaction energy. The information found by the critical molecular weight experiments and in the literature was used to constrain the possible B_{ij} values in this study. For each set of interaction energies within the constraints, the program first determines the curve represented by the interaction energies, as defined by Eq. (2). Then, the sum of the orthogonal distance between this curve and the data points along the miscibility border is calculated. The program also includes an arbitrary penalty for each data point on the wrong side of the boundary, such as a miscible data point located in the immiscible region. The sum of the orthogonal distances and the penalties comprise an objective function. The program determines the set of B_{ij} values for which this objective function is minimized.

The five B_{ij} values found by fitting the theory independently to the data for both blend systems are shown in Table 7. The corresponding values of ΔP_{ij}* computed from these values using Eq. (5) are also shown. Both systems yield a value of $B_{MMA/AN} = 4.51$ cal/cm^3 which agrees well with the literature results shown in Fig. 2(b). For the S/AN interaction, the EA results lead to a value of 7.13 cal/cm^3 while the nBA results give a slightly lower value of 7.05 cal/cm^3, both of which fall within the range of prior results as seen in Fig. 2(a). Table 7 also shows the interaction energies for EA and for nBA with S, AN and MMA. The trend of these values with repeat unit structures will be discussed in a subsequent section. The confidence limits for the calculated interaction

Table 7
Interaction energies (cal/cm^3) at 120°C

Interaction pair	MMA-EA/SAN		MMA-nBA/SAN		Confidence limits for B_{ij} (cal/cm^3)
	ΔP^*_{ij}	B_{ij}	ΔP^*_{ij}	B_{ij}	
S/MMA	0.23	0.22	0.23	0.22	± 0.02
MMA/AN	4.55	4.51	4.55	4.51	± 0.33
S/AN	7.49	7.13	7.40	7.05	± 0.43
MMA/EA	−0.11	0.11			± 0.10
S/EA	0.64	0.86			± 0.10
EA/AN	4.43	5.01			± 0.11
MMA/nBA			0.31	0.45	± 0.05
S/nBA			0.04	0.28	± 0.05
nBA/AN			6.29	6.63	± 0.05

energies, given in Table 7, were found by adjusting each interaction parameter and determining the limit where a fit to the miscibility data could be found by changing the other parameters [36].

7. Phase separation behavior

Another method of gaining information about interaction energies is to analyze the observed phase diagram using the lattice-fluid theory. New experimental PVT data for PnBA developed for this purpose are reported in Table 8. The Sanchez–Lacombe characteristic parameters deduced from these data are listed in Table 4 along with the other relevant characteristic parameters given in the literature.

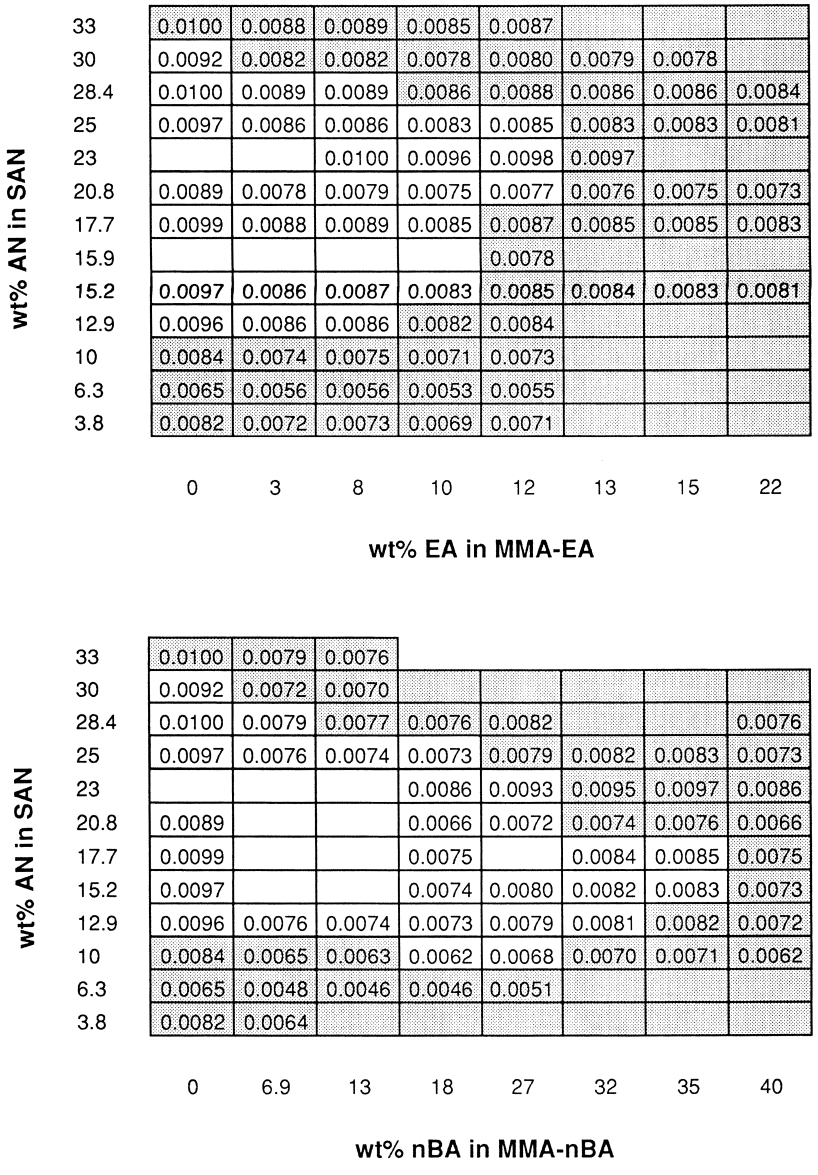

Fig. 6. B_{crit} values (cal/cm^3) as a function of blend composition: (a) MMA-EA/SAN; (b) MMA-nBA/SAN. Shaded boxes correspond to immiscible blend compositions and unshaded boxes correspond to miscible blends.

Table 8
Specific volume (cm^3/g) of PnBA as a function of pressure and temperature

P (MPa)	T (°C)						
	30	60	90	120	150	180	210
10	0.9137	0.9356	0.9546	0.9745	0.9976	1.0192	1.0415
20	0.9076	0.9285	0.9468	0.9654	0.9866	1.0067	1.0266
30	0.9026	0.9227	0.9406	0.9581	0.9786	–	1.0161
40	0.8980	0.9177	0.9347	0.9515	0.9710	0.9888	1.0066
50	0.8939	0.9127	0.9292	0.9453	0.9641	0.9813	0.9982
60	0.8899	0.9081	0.9242	0.9396	0.9576	0.9743	0.9906
70	0.8861	0.9038	0.9194	0.9343	0.9516	0.9680	0.9834
80	0.8825	0.8992	0.9149	0.9296	0.9455	0.9614	0.9765
90	0.8788	0.8955	0.9106	0.9246	0.9408	0.9556	0.9704
100	0.8753	0.8918	0.9064	0.9204	0.9358	0.9502	0.9648
110	0.8722	0.8885	0.9026	0.9160	0.9309	0.9452	0.9593
120	0.8691	0.8850	0.8987	0.9118	0.9266	0.9404	0.9539
130	0.8663	0.8817	0.8950	0.9080	0.9221	0.9359	0.9488
140	0.8633	0.8789	0.8917	0.9040	0.9182	0.9311	0.9441
150	0.8604	0.8755	0.8884	0.9004	0.9140	0.9271	0.9394
160	0.8577	0.8724	0.8853	0.8966	0.9102	0.9230	0.9352
170	0.8553	0.8698	0.8822	0.8934	0.9065	0.9189	0.9309
180	0.8524	0.8669	0.8788	0.8900	0.9030	0.9150	0.9266
190	0.8500	0.8641	0.8758	0.8866	0.8993	0.9113	0.9228
200	0.8476	–	0.8729	0.8835	0.8959	0.9077	0.9187

Only two of the MMA-EA/SAN blends and one MMA-nBA/SAN blend were found to exhibit LCST behavior within the accessible temperature ranges between the glass transition and the thermal degradation limit. The experimental phase separation temperatures are shown in Table 9. The calculated spinodal temperatures for each of these blends predicted by the interaction energies found from the copolymer miscibility maps are also in Table 9. While the experimental phase separation temperatures do not necessarily correspond to the spinodal temperatures, they are expected to follow a similar trend.

The experimental phase separation temperature for the MMA-EA3/SAN30 blend was found to be between 190°C and 200°C. This is similar to the spinodal temperature of 190°C predicted by the interaction energies determined from the miscibility map. The MMA-EA8/SAN28 blend exhibited phase separation between 120°C and 130°C, which is close to the predicted spinodal temperature of 137°C. The only butyl acrylate copolymer to show any phase separation was MMA-nBA7; its blend with SAN28 phase separated between 180°C and 185°C. This also is similar to the spinodal temperature of 183°C predicted by the interaction energies. Thus, all of the experimental phase separation temperatures are close to those predicted by the interaction energies from the isothermal miscibility maps.

Table 9
Predicted spinodal temperatures and experimental phase separation temperatures for blends in this study

Blend (50/50 wt%)	Predicted spinodal temperature (°C)	Experimental phase separation temperature (°C)
MMA-EA3/SAN30	190	190–200
MMA-EA8/SAN28	137	120–130
MMA-nBA7/SAN28	183	180–185

8. Trends in interaction energies

The interaction energies for various methacrylate and acrylate repeat units, including ethyl methacrylate (EMA), *n*-propyl methacrylate (nPMA), and *n*-butyl methacrylate (nBMA), with styrene, acrylonitrile, and methyl methacrylate repeat units are shown in Table 10. This table includes interaction energies from previous studies of blends of MMA-X copolymers with SAN copolymers, where X = tert-butyl methacrylate (tBMA) [9,10], phenyl methacrylate (PhMA) [9,32], and cyclohexyl methacrylate (CHMA) [9,32]. For consistency, these data have been reevaluated via the computer program described previously using the parameters fixed in this study; the recalculated interaction energies are included in Table 10. The corresponding miscibility maps are shown in Fig. 7. The interaction energies determined here differ only slightly from those determined previously; as seen in Table 10, most of these interaction energies are within or just outside of the range of values found formerly. DiPaolo-Baranyi and Degré [37] blended a high molecular weight poly(*n*-butyl methacrylate) (PnBMA) with two monodisperse PS homopolymers, one of high molecular weight and the other of low molecular weight. The blend with the PS of higher molecular weight was found to be immiscible, while that with the lower molecular weight PS was miscible. These data were analyzed

using Eq. (3) to obtain the range of values listed in Table 10 for $B_{S/nBMA}$. Similarly, Cowie et al. [35] blended PMMA polymers of various molecular weights with poly(methyl acrylate) (PMA) and poly(ethyl acrylate) (PEA) of various molecular weights. Analysis of the reported phase behavior of these blends using Eq. (3) gives $0.19 < B_{MMA/MA} < 0.22$ and $B_{MMA/EA} = 0.13$ cal/cm^3, which differ slightly from the values reported by Cowie et al. [35]

The first section of Table 10 deals with the interaction of MMA units with other methacrylate and acrylate units. The interaction energy of MMA with each of the methacrylates and acrylates of interest here is positive. The interaction of MMA with each of these acrylates is a small, positive value. As the length of the pendant *n*-alkyl group in the acrylate repeat unit increases, the interaction energy of the acrylate with MMA initially decreases then increases; the interaction with EA has the smallest value. The interaction energies of MMA with methacrylates listed in Table 10 are all larger than the interaction energies of MMA with acrylates. Other values for the interaction of MMA with some *n*-alkyl methacrylates [38,39] are not given in Table 10 because the methods employed to evaluate them are not as reliable as those used here. The interaction energy for MMA with tBMA is larger than that with CHMA which is larger than that with PhMA.

The interaction energies for the acrylonitrile unit with the methacrylate and acrylate units shown in Table 10 are all positive and much larger than those for methyl methacrylate units with other methacrylate and acrylate units. The

Table 10
Interaction energy densities (cal/cm^3)of methacrylates and acrylates

Interaction pair	B	ΔP^*	T (°C)	Reference
MMA-tBMA	1.35		130	this study[a]
	1.36–1.67		130	[9]
MMA-CHMA	0.73		130	this study[a]
	0.80–0.87		130	[9]
MMA-PhMA	0.23		130	this study[a]
	0.20–0.30		130	[9]
MMA-MA	0.19–0.22		30	[35][b]
MMA-EA	0.11	− 0.11	120	this study
	0.13		30	[35][b]
MMA-nBA	0.45	0.31	120	this study
AN-MMA	4.51	4.55	120	this study
AN-EMA	5.33		30	[29]
AN-nPMA	5.85		30	[29]
AN-tBMA	6.42		130	this study[a]
	6.05–6.40		130	[9]
AN-CHMA	6.66		130	this study[a]
	6.56–6.90		130	[9]
AN-PhMA	4.47		130	this study[a]
	4.35–4.42		130	[9]
AN-EA	5.01	4.43	120	this study
AN-nBA	6.63	6.29	120	this study
S-MMA	0.22	0.23	120	[30]
S-EMA	− 0.0361	− 0.061	30	[29]
S-nPMA	− 0.0309	− 0.151	30	[29]
S-nBMA	0.01–0.27		140	[37][c]
S-tBMA	0.75		130	this study[a]
	0.97–1.01		130	[9]
S-CHMA	− 0.03		130	[9]
S-PhMA	0.20		130	this study[a]
	0.33–0.39		130	[9]
S-EA	0.86	0.64	120	this study
S-nBA	0.28	0.04	120	this study

[a]Recalculated from data in Ref. [9].
[b]Recalculated from data in Ref. [35].
[c]Calculated from data in Ref. [37].

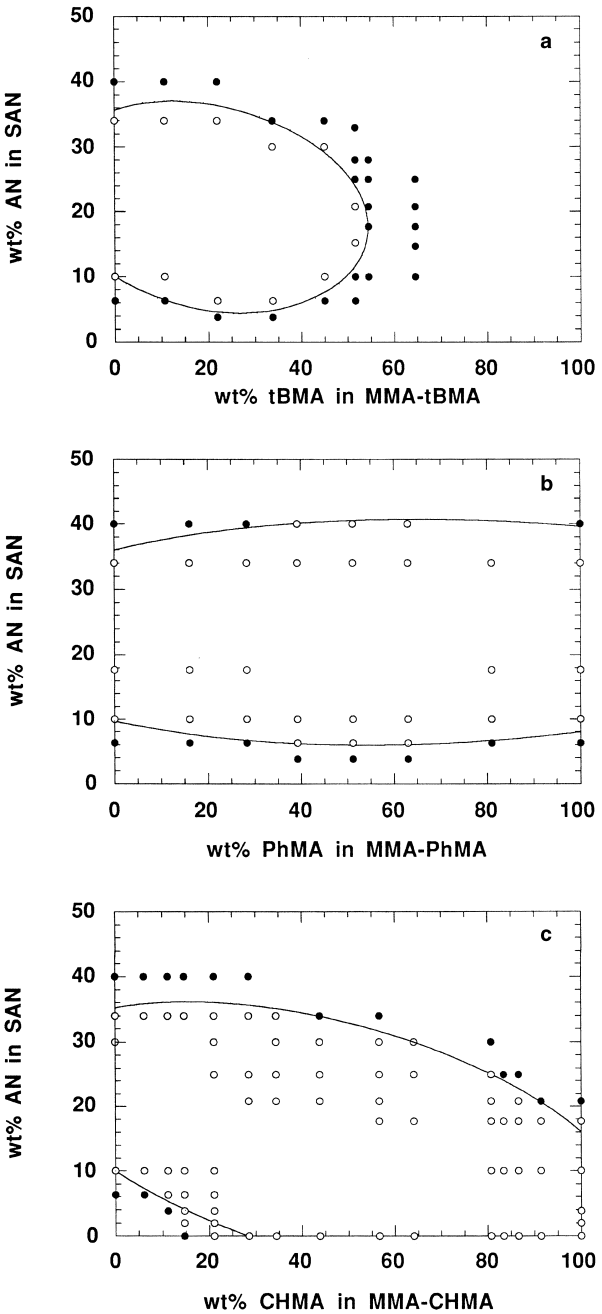

Fig. 7. Copolymer miscibility map at 130°C for 50/50 wt% blends of SAN copolymers with: (a) MMA-tBMA; (b) MMA-PhMA; and (c) MMA-CHMA copolymers: (◦) miscible; (•) immiscible. Data taken from Ref. [9]. The solid curve was calculated from the B_{ij} set obtained from the best fit of the miscibility map (see Table 10 for values).

interaction energy of AN with nBA is greater than that with EA. The interaction energies for AN with *n*-alkyl methacrylates increase with increasing *n*-alkyl group length. The interaction energy of AN with tBMA is greater than with the *n*-alkyl methacrylates, and the interaction energy of AN with CHMA is even greater. The interaction energy of AN with PhMA, the only repeat unit with an aromatic group, is the smallest of the interaction energies with AN listed in Table 10.

The last section of Table 10 lists the interaction energies of styrene units with several methacrylate and acrylate repeat units. The absolute values of all of these interaction energies are relatively small compared to the interaction of these units with acrylonitrile; most are positive, but a few are slightly negative. The interaction energies of styrene with nBA is less than with EA, but both $B_{S/EA}$ and $B_{S/nBA}$ are positive. Brannock et al. [29] proposed the following trend for the interaction of styrene with methacrylates containing *n*-alkyl groups: $B_{S/MMA}$ is slightly positive, but as the length of the *n*-alkyl group increases, the interaction energy decreases to negative values, then increases again to positive values after reaching a minimum. The values in Table 10 are consistent with this trend, with the S/EMA interaction representing the minimum value. The branching of butyl methacrylate (tBMA vs nBMA) appears to increase the interaction energy with styrene. The interaction energy of styrene with CHMA is a small negative number, but the interaction energy with PhMA is positive.

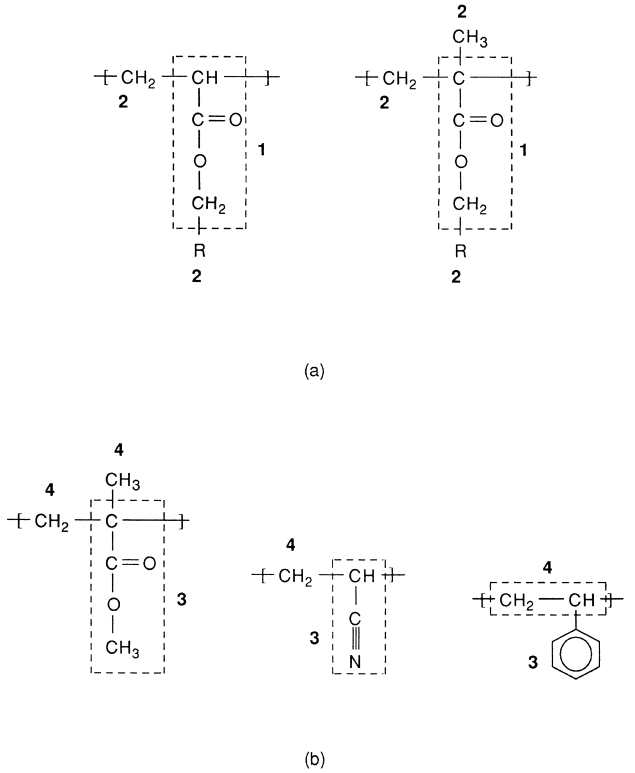

Fig. 8. Structures of polymer repeat units divided into electroneutral groups as indicated by the dashed lines. The bold numbers are assigned to represent a particular group in the binary interaction energy equation [Eq. (2)]. The repeat units represented are: (a) acrylates and methacrylates; and (b) methyl methacrylate, acrylonitrile, and styrene.

Table 10 shows that the interaction energy for methacrylates or acrylates with styrene, acrylonitrile and methyl methacrylate depend on the nature of the pendant alkyl group. In some cases it is possible to rationalize the trends in B_{ij} values using the method developed by Ziaee and Paul [40–42] which involves dividing monomer repeat units into smaller groups and using the binary interaction model to develop an expression for the interaction energy density for a monomer pair. The monomer repeat units were divided into electroneutral groups as suggested by Wu and Sandler [43]; the repeat units and their divisions are shown in Fig. 8. The following discussion concerns the interaction energy between a repeat unit in Fig. 8(a) with a repeat unit in Fig. 8(b). Since each of the repeat units consists of two groups, the interaction energy between the two monomer units can be represented by Eq. (2), where now ϕ_i' is the volume fraction of group i in repeat unit A, ϕ_j'' is the volume fraction of group j in repeat unit B, and B_{ij} is the interaction between groups i and j. The bold numbers in Fig. 8 indicate the subscript assigned to each group which will be used in the binary interaction model. Because some of the interaction energies between these groups are known, this procedure can allow a semi-quantitative analysis of the trends in interaction energy seen in Table 10.

Using the procedure described above, acrylate and methacrylate repeat units can be divided as shown in Fig. 8(a) where subunit 1 includes the ester group and subunit 2 are the alkyl groups. The divisions of the particular repeat unit of MMA are shown in Fig. 8(b). The acrylonitrile repeat unit can be divided into the two groups shown in Fig. 8(b), where the cyano group and the adjacent alkyl group form subunit 3 and the remaining alkyl group is subunit 4. Also in Fig. 8(b) is the repeat unit of styrene, which is divided into its aromatic and alkyl components. It is assumed in all calculations that the interaction between alkyl groups is zero, i.e. $B_{24} = 0$. It is also assumed that the interaction between the units that include the ester group of the acrylates and the ester group of the methacrylates, which differ only by an alkyl hydrogen, is zero; thus all ester group/alkyl group interactions are equal, i.e. $B_{12} = B_{14}$.

The interaction between MMA and acrylates provides the simplest case for this type of analysis. Since each of these repeat units consists of similar ester and alkyl groups, the assumption that all ester/alkyl interactions are equal includes four group interactions: $B_{12} = B_{14} = B_{23} = B_{34}$. Also, the assumption that the interaction between the methacrylate ester group and the acrylate ester group is zero gives $B_{13} = 0$. These assumptions combined with Eq. (2) lead to

$$B = B_{12}(\phi_1'\phi_4'' + \phi_2'\phi_3'' - \phi_1'\phi_2' - \phi_3''\phi_4''). \quad (6)$$

Although the value of B_{12} is not known, the volume fractions in parenthesis on the right side of Eq. (6) can be calculated using Van der Waals volumes. Since B_{12} is assumed to be constant, the terms in parenthesis for the different

acrylates should reflect the variations in the overall interaction energy values. Calculating the appropriate volume fractions shows that the value in parenthesis is a small positive number for $B_{MMA/MA}$, is equal to zero for $B_{MMA/EA}$ and is another small positive number for $B_{MMA/nBA}$. Obviously, since $B_{MMA/EA}$ is not zero, this method cannot be used to determine exact quantities. However, it is interesting to see the same general trend in these quantities as is seen in the overall interaction energies; the values are positive and have a minimum value corresponding to the MMA/EA interaction. The semi-quantitative analysis is not provided for the interactions between MMA and methacrylates as the pendant groups of the methacrylates in this section of the table do not have the *n*-alkyl group structure. Thus, it is likely that the differences in the interactions involving a tertiary butyl group, cyclohexyl group and aromatic group are significant and do not allow the same monomer group divisions and simplifying assumptions.

The interaction energies between methacrylates and acrylates with acrylonitrile can be analyzed similarly. Using the general simplifying assumptions discussed above with Eq. (2) gives

$$B = B_{13}\phi_1'\phi_3'' + B_{14}\phi_1'(\phi_4'' - \phi_2') + B_{23}\phi_2'\phi_3'' - B_{34}\phi_3''\phi_4''. \quad (7)$$

Again this analysis was limited to the *n*-alkyl acrylates and methacrylates. Ziaee and Paul [42] found the interaction between the cyano containing group (subunit 3) and a non-bonded alkyl group (subunit 2) to be strongly repulsive, or $B_{23} = 23.5 \pm 3.8$ cal/cm^3; whereas, the interaction between the cyano containing group and a bonded alkyl group (subunit 4) to be much smaller: $B_{34} = -0.391 \pm 2.390$ cal/cm^3. The intramolecular cyano/alkyl term of Eq. (7), $B_{34}\phi_3''\phi_4''$, is a small positive number and depends only upon the acrylonitrile repeat unit. It will not vary with different acrylate and methacrylate repeat units. The coefficients for B_{13} are small positive values while the coefficients for B_{14} are small negative numbers; however, both coefficients have decreasing values as the length of the pendant *n*-alkyl group increases, for both the acrylates and methacrylates. This suggests that if B_{13} and B_{14} are positive values, as they likely are, these terms decrease as the length of the *n*-alkyl group increases, which is the opposite trend seen in the overall interaction energies. The coefficients for B_{23} are positive and increase with increasing *n*-alkyl group length. Since B_{23} has been determined to be a large positive number, it is known that this intermolecular cyano/alkyl term also increases with the length of the alkyl group. Because this term is large and is the only term that follows the same trend as the overall interaction energies between the monomer pairs, it suggests this is the dominant term for these interaction energies.

The same analysis can be performed for the interaction energies for styrene with methacrylates and acrylates. Assuming the alkyl/aromatic ring interactions are equal ($B_{23} = B_{34}$) along with the general assumptions stated earlier leads to the following equation

$$B = B_{13}\phi_1'\phi_3'' + B_{14}\phi_1'(\phi_4'' - \phi_2') + B_{23}\phi_3''(\phi_2'\phi_4''). \quad (8)$$

Ziaee and Paul [40] determined that the interaction energy for a phenyl group and an alkyl group is positive: $B_{23} = 7.74$ cal/cm^3. With these interaction energies, the terms in Eq. (8) show different trends for acrylates and methacrylates. The calculations for the interaction energies of styrene with the two acrylates show the coefficients for B_{23} are small positive values and the value for nBA is larger than that for EA. As B_{23} is known to be a positive number, this alkyl/aromatic ring term is greater for nBA than for EA. The coefficients for B_{13} are positive and those for B_{14} are negative, but both are smaller for nBA than EA. Again, assuming the these interaction energies are positive, these terms exhibit the same trend as the overall interaction energies. For the interaction energies of styrene with methacrylates the B_{23} and B_{13} terms show the same trends as with the acrylates; both terms are positive and the B_{23} term increases with increasing length of the *n*-alkyl group while the B_{13} term decreases with increasing *n*-alkyl group length. However, for the methacrylate interactions, the B_{14} terms are negative and initially decrease then increase as the length of the *n*-alkyl group increases, with the minimum value corresponding to the S/nPMA interaction. This trend is similar to that of the overall interaction energies, which decrease then increase as the length of the *n*-alkyl group increases, but the minimum value for the overall interaction energies corresponds to the S/EMA interaction. Thus, there is not one group interaction, or term in Eq. (8), which clearly dominates the others in determining the overall interaction energies for styrene with methacrylates.

9. Summary

The miscibility regions for styrene–acrylonitrile copolymers with methyl methacrylate copolymers containing ethyl acrylate and *n*-butyl acrylate were determined. The miscibility window for PMMA with SAN copolymers is well-defined [1–7] and has a larger miscibility range than the MMA-acrylate copolymers have with SAN. The miscibility region for the *n*-butyl acrylate copolymers is larger than that for the ethyl acrylate copolymers. The copolymer miscibility maps were used, along with other information, to determine the relevant interaction energy densities. The MMA/styrene interaction, $B_{S/MMA}$, was equated to 0.22 cal/cm^3 based upon information in the literature [30]. The remaining interaction energy densities were determined using the critical molecular weight method and data from the miscibility maps in conjunction with the Flory–Huggins theory and the binary interaction model. A computer program was used to facilitate this analysis. All B_{ij} values were found to be positive; these interaction energy densities are consistent with values reported previously, where comparisons can be made. A few miscible blends exhibited phase separation upon heating. Spinodal

temperatures predicted from the lattice-fluid theory using these interaction energies are similar to the experimental phase separation temperatures. Table 7 lists the interaction energy densities evaluated in this study, and Table 10 includes interaction energy densities obtained from other sources.

Acknowledgements

This research was funded by National Science Foundation grant numbers DMR 92-15926 and DMR 97-26484.

References

[1] Chiou JS, Paul DR, Barlow JW. Polymer 1982;23:1543.
[2] Fowler ME, Barlow JW, Paul DR. Polymer 1987;28:1177.
[3] Cowie JMG, Lath D. Makromol Chem, Macromol Symp 1988;16:103.
[4] Suess J, Kressler J, Kammer HW. Polymer 1987;28:957.
[5] Kressler J, Kammer HW, Klostermann K. Polym Bull 1986;15:113.
[6] Nishimoto M, Keskkula H, Paul DR. Polymer 1989;30:1279.
[7] Nishimoto M, Keskkula H, Paul DR. Macromolecules 1990;23:3633.
[8] Gan PP, Paul DR. Polymer 1994;35:3513.
[9] Gan PP. PhD dissertation, The University of Texas at Austin, 1994.
[10] Paul DR. Pure Appl Chem 1995;67:977.
[11] Huggins ML. J Chem Phys 1941;9:440.
[12] Flory PJ. J Chem Phys 1942;10:51.
[13] Paul DR, Barlow JW. Polymer 1984;25:487.
[14] Kambour RP, Bendler JT, Bopp RC. Macromolecules 1983;16:753.
[15] tenBrinke G, Oudhius L, Ellis TS. Thermochim Acta 1994;238:15.
[16] Callaghan TA, Paul DR. Macromolecules 1993;28:2439.
[17] Callaghan TA, Paul DR. J Polym Sci: Part B: Polym Phys 1994;32:1813.
[18] Lacombe RH, Sanchez IC. J Phys Chem 1976;80:2568.
[19] Sanchez IC, Lacombe RH. J Phys Chem 1976;80:2353.
[20] Sanchez IC, Lacombe RHJ. Polym Sci, Polym Lett 1977;15:71.
[21] Sanchez IC, Lacombe RH. Macromolecules 1978;11:1145.
[22] Sanchez IC. In: Meyers RA, editor. Encyclopedia of physical science and technology, vol. 11. New York: Academic Press, 1987.
[23] Callaghan TA. PhD dissertation, The University of Texas at Austin, 1992.
[24] Kim CK, Paul DR. Polymer 1992;33:1630.
[25] Fukuda T, Inagaki H. Pure Appl Chem 1983;55:1541.
[26] Fukuda T, Nagata M, Inagaki H. Macromolecules 1984;17:548.
[27] Fukuda T, Nagata M, Inagaki H. Macromolecules 1986;19:1411.
[28] Russell TP. Macromolecules 1993;26:5819.
[29] Brannock GR, Barlow JW, Paul DR. J Polym Sci: Part B: Polym Phys 1991;29:413.
[30] Gan PP, Paul DR. Polymer 1994;35:1487.
[31] Gan PP, Paul DR. J Appl Polym Sci 1994;54:317.
[32] Nishimoto M, Takami Y, Tohara A, Kasahara H. Polymer 1995;36:1441.
[33] Kim CK, Paul DR. Polymer 1992;33:2089.
[34] Rodgers PA. J Appl Polym Sci 1993;48:1061.
[35] Cowie JMG, Ferguson R, Fernandez MD, Fernandez MJ, McEwen IJ. Macromolecules 1992;25:3170.
[36] Merfeld GD, Paul DR. Polymer 1998;39:1999.
[37] DiPaola-Baranyi G, Degre P. Macromolecules 1981;14:1456.
[38] Goh S, Siow K. Polym Bull 1988;20:393.
[39] Shiomi T, Tohyama M, Endo M, Sato T, Imai K. J Polym Sci 1996;34:2599.
[40] Ziaee S, Paul DR. J Polym Sci: Part B: Polym Phys 1996;34:2641.
[41] Ziaee S, Paul DR. J Polym Sci: Part B: Polym Phys 1997;35:489.
[42] Ziaee S, Paul DR. J Polym Sci: Part B: Polym Phys 1997;35:831.
[43] Wu HS, Sandler SI. Indust Engng Chem Res 1991;30:881.